Journal of Magnetic Resonance 203 (2010) 247–252

Contents lists available at ScienceDirect

Journal of Magnetic Resonance

journal homepage: www.elsevier.com/locate/jmr

Self-refocused slice selection by magic echo DANTE with 270° flipping Gaussian RF modulation

Hidefumi Masumoto [a], Takeyuki Hashimoto [c], Shigeru Matsui [a,b,*]

[a] Graduate School of Pure and Applied Sciences, University of Tsukuba, Tsukuba, Ibaraki 305-8573, Japan
[b] Institute of Applied Physics, University of Tsukuba, Tsukuba, Ibaraki 305-8573, Japan
[c] Department of Information Technology, Yokohama Soei Junior College, Yokohama, Kanagawa 226-0015, Japan

ARTICLE INFO

Article history:
Received 18 September 2009
Revised 1 January 2010
Available online 11 January 2010

Keywords:
Self-refocused slice selection
MRI
DANTE
Magic echo
Line narrowing

ABSTRACT

The method of slice selection proposed for solid-state MRI by combining DANTE selective excitation with magic echo (ME) line narrowing requires a rephasing period ca. 0.6 times the DANTE excitation period. The added rephasing period results in a significant loss of sensitivity due to transverse relaxation. To solve the sensitivity problem, we make use of the self-refocusing effect of the 270° Gaussian-shaped soft pulse by introducing a 270° flipping Gaussian modulation to the ME DANTE method. This eliminates the rephasing period. The utility of the improved method is demonstrated by experiments performed on test samples of adamantane and polycarbonate.

1. Introduction

We have recently described the method of slice selection in solid-state MRI [1]. The method combines the DANTE selective excitation [2] with magic echo (ME) line narrowing [3–13] without introducing significant interference between the DANTE and ME sequences. It has enabled tailoring the slice profile for the first time in solid-state MRI by introducing a suitable amplitude modulation to the DANTE RF pulses, e.g., a sinc modulation for achieving an ideal rectangular profile.

The DANTE RF excitation made in the presence of the field gradient is necessarily associated with dephasing of the excited signal. The dephasing is usually recovered nearly perfectly by the subsequent application of the inverted field gradient [14]. The unrecoverable dephasing can be related to the nonlinear response of the spin system to the DANTE excitation [15]. The rephasing period following the excitation can be ca. 0.6 times as long as the excitation period, resulting in loss of sensitivity due to transverse relaxation during the added rephasing period. The loss of sensitivity is small in liquid-state MRI, since the dephasing period is usually much shorter than the transverse relaxation time [15]. On the other hand, the loss is significant in solid-state MRI where the transverse relaxation governed by the ME line narrowing sequence is not satisfactorily slow. In most organic solids, the signal decay times obtained by the ME line narrowing (TREV8) are in the range of 1–5 ms; each decay time is about the same as the corresponding rephasing period. For example, the rephasing period can be 1.3 ms long in our ME DANTE experiments.

A simple and efficient solution to such a problem in sensitivity is to rely on the self-refocusing effect demonstrated in certain selective excitations [15]. Among these, we focus on the 270° Gaussian-shaped soft pulse successfully applied to selective 2D exchange spectroscopy by Emsley and Bodenhausen [16]. To make use of the self-refocusing effect of the 270° Gaussian pulse in the ME DANTE slice selection, we modulate the amplitudes of the DANTE RF hard pulses so that the envelope of the hard pulses becomes Gaussian.

Here, we demonstrate by numerical simulations and preliminary experiments that the self-refocused ME DANTE slice selection by 270° flipping Gaussian modulation can easily be implemented and is indeed useful.

2. The conventional and self-refocused ME DANTE method

The upper sequence in Fig. 1 shows the pulse sequence of the previously proposed ME DANTE method, which is now briefly reviewed. The portion of the DANTE sequence for slice selection consists of regularly spaced N short RF pulses and a field gradient G. The on resonance flip angle of each pulse is defined by α_i ($i = 1, 2, 3, \ldots, N$) and the sum of the flip angles is fixed at 90°. The regular spacing of the DANTE hard-pulse sequence makes it ideally suited for the combination with the ME sequence which is cyclic. For combining the DANTE sequence with the ME line narrowing sequence without

* Corresponding author. Address: Graduate School of Pure and Applied Sciences, University of Tsukuba, Tsukuba, Ibaraki 305-8573, Japan. Fax: +81 29 853 5205.
E-mail address: matsui@bk.tsukuba.ac.jp (S. Matsui).

1090-7807/$ - see front matter © 2010 Elsevier Inc. All rights reserved.
doi:10.1016/j.jmr.2010.01.002

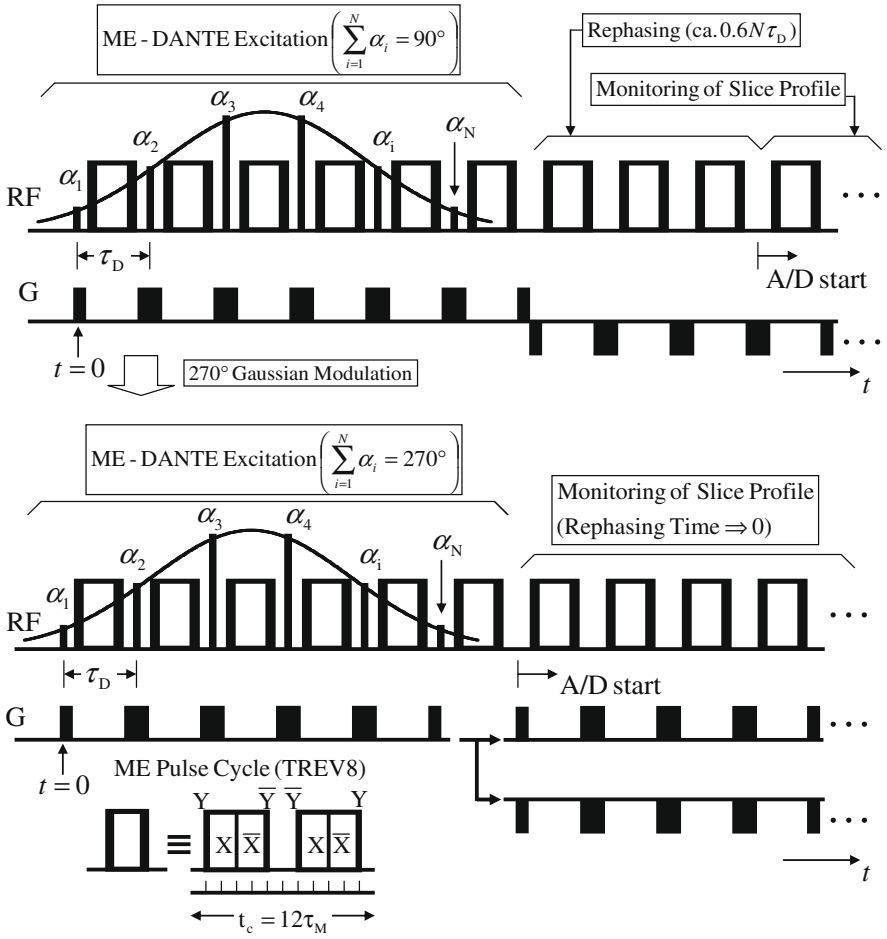

Fig. 1. Pulse sequences for the conventional (upper) and self-refocused (lower) ME DANTE method of slice selection. The upper sequence consists of three periods: the ME DANTE excitation, rephasing, and monitoring period. During the ME DANTE excitation period, N hard RF pulses with flip angles α_i ($i = 1, 2, 3, \ldots, N$) are applied every pulse cycle of TREV8. Field gradient pulses G are applied for transforming the frequency response of the ME DANTE RF pulses to the spatial response. The field gradient G is inverted for rephasing transverse magnetization dephased during the ME DANTE excitation period. The profile of selected slice is then monitored. The total flip angle of the DANTE pulses is set at 90°. Note that in the lower sequence, the rephasing period is eliminated and further the total flip angle is changed to 270°. The envelope of the DANTE RF pulses is modulated by a Gaussian function. The α_i pulse amplitudes are depicted exaggerated; the maximum amplitude is the same as that of 90° pulses in the ME sequence.

lowering the line narrowing efficiency, it is necessary to apply the DANTE RF pulses at the ME peaks where the time evolution of the spin system is ideally free from the dipolar interaction. However, in real experiments the dipolar-free time evolution is hindered mainly by the sandwiching $90^{\circ}_{\pm y}$ pulses which are not sufficiently short [13]. The TREV8 [4] was employed as the ME pulse cycle. The cycle time $t_c = 12\tau_M$ ($\tau_M = 30$ μs) was set equal to the DANTE pulse spacing $\tau_D = 360$ μs. All the DANTE RF pulses are applied along the x axis in the rotating frame.

The ME DANTE excitation is followed by the ME sequence with reversed gradient pulses for rephasing the signal, similarly as in the soft RF pulse excitation commonly used for liquid-state MRI [14]. When the total flip angle of DANTE pulses is fixed at 90°, the rephasing period is ca. $0.6N\tau_D$ long following the excitation. This nonnegligible rephasing period leads to the loss of sensitivity due to transverse relaxation during the rephasing period. In the lower sequence, however, the total flip angle of the DANTE pulses is changed to 270° for achieving the self-refocusing, allowing the elimination of the rephasing period.

The lower sequence consists of two versions where the polarity of the field gradient is reversed. Since the rephasing achieved by the 270° DANTE is not perfect, two FID signals taken with opposite gradient polarities are to be observed for obtaining the correct profile. The Fourier transforms of the FID's are summed up appropriately. On the other hand, since the rephasing is more complete in the case of the 90° DANTE, such alternation of gradient is not necessary to give the nearly correct profiles [1].

It should be noted that since the more complete rephasing achieved in the 90° DANTE can be obtained at the expense of the added rephasing period, the overall advantage of the 270° DANTE remains unaffected by the problem of non-perfect rephasing.

3. Simulation of self-refocused DANTE

Emsley and Bodenhausen [16] have already reported magnetization trajectories calculated for a 270° Gaussian soft pulse using numerical solutions of the Bloch equations, visualizing the self-refocusing effect of the 270° pulse. (The self-refocusing effect has also been pointed out by Freeman et al. [17].) Further, they have calculated the amplitude response and the phase behavior for the 270° pulse as a function of the offset frequency. However, since no simulation results seem to have been published for the 270° Gaussian-modulated DANTE, we have carried out similar numerical simulations based on the Bloch equations. The Gaussian modulation function is defined as

$$G_m(t) = G_0 \exp\left(-g\left(t - \frac{N-1}{2}\tau_D\right)^2\right) \quad (1)$$

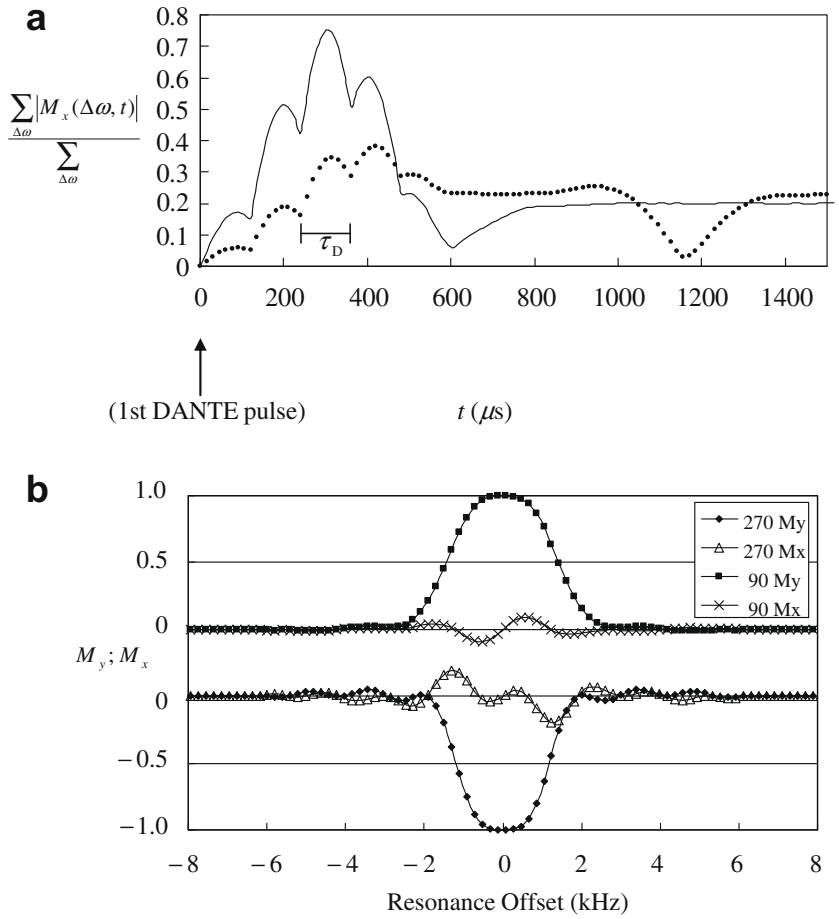

Fig. 2. Simulation results of the DANTE using the 270° and 90° flipping Gaussian modulation. Note that in the simulation, unlike the ME DANTE shown in Fig. 1, only N hard RF pulses with flip angles α_i ($i = 1, 2, 3, \ldots, N$; $N = 6$) are applied every $\tau_D = 120$ μs in the continuous presence of the gradient G. Immediately after this excitation time, the gradient is inverted for rephasing the signal in the case of 90° flipping. No rephasing period is necessary for 270° flipping. (a) Plots of the normalized sum of the absolute value of M_x over the centerband frequency region $\sum_{\Delta\omega}|M_x(\Delta\omega, t)|/\sum_{\Delta\omega}$ as a function of the excitation time ($t = 0$ at the 1st DANTE pulse, see Fig. 1). Rephasing occurs with decreasing sum of $|M_x|$ and dephasing with increasing sum of $|M_x|$. The curve represented by solid line was obtained by the 270° flipping DANTE. The curve depicted by dotted line was obtained by the 90° flipping DANTE. For both curves, the overall rephasing is not complete; however, minima are observed at $t = 600$ and 1162 μs. Note that the minimum values depend on the curves (0.059 at $t = 600$ μs and 0.029 at $t = 1162$ μs). The value of 1162 μs is given as $(1 + 0.61)\, N\tau_D$. The factor 0.61 is obtained for the Gaussian modulation while it was 0.58 for the sinc modulation [1]. This factor for the length of the rephasing period relative to that of the excitation period depends on the type of the DANTE RF modulation. (b) Plots of M_y (profiles) and M_x calculated at $t = 600$ (lower) and 1162 μs (upper) as a function of resonance offset. The lower profile is well selected with no rephasing time. The sidelobes of the lower profile is slightly larger than those of upper profile. Plots of M_x represent a measure of incomplete rephasing. Relaxation effects were neglected for the results shown.

where g determines the width at half maximum and G_0 is determined automatically by the total flip angle of DANTE RF pulses and the factor g.

Emsley and Bodenhausen [16] have defined the useful region of excitation by a small offset at which the amplitude response drops to 90% of its maximum value. The phase variation within this region was less than about 45°. In the case of slice selection, however, a much larger region of excitation extending from on resonance to far off resonance must be used for defining a slice profile. As a result, the region relevant to our simulation was taken over the centerband, which was $\pm 1/2\tau_D$ wide, and overall rephasing was evaluated.

The τ_D value was set at 120 μs while it was 360 μs for the ME DANTE experiments (see Fig. 1). This is related to the scaling factor 1/3 of the ME sequence. The effect of the field gradient is scaled down by the factor in the ME DANTE experiments. An obvious way of taking into account the scaling is to use the field gradient three times stronger than that in the DANTE experiments while keeping the τ_D value at 120 μs. An alternative way is to increase the τ_D value three times compared to that in the DANTE experiments while using the same gradient amplitude as in the DANTE experiments. We took the latter way for experimental convenience.

The results are summarized in Fig. 2. Fig. 2a shows the degree of dephasing and rephasing obtained by calculating the out-of-phase component of the transverse magnetization, $M_x = M_{xy} \sin \Phi$, as a function of the DANTE excitation time ($t = 0$ at the 1st DANTE pulse, see Fig. 1). The curve depicted by solid line shows the result of the 270° Gaussian modulation and the curve represented by dotted line the result of the conventional 90° Gaussian modulation followed by the separate rephasing. Plotted is the normalized sum of the absolute value of M_x over the centerband frequency region $\sum_{\Delta\omega}|M_x(\Delta\omega, t)|/\sum_{\Delta\omega}$. Rephasing occurs with decreasing sum of $|M_x|$ and dephasing with increasing sum of $|M_x|$. The curve depicted by solid line clearly shows overall dephasing during the former half of the excitation and overall rephasing during the latter half, though finer dephasing and to a less degree, rephasing occurs after each DANTE pulse. It can also be seen from the curve that the overall rephasing is not perfect, since the value of $\sum_{\Delta\omega}|M_x(\Delta\omega, t)|/\sum_{\Delta\omega}$ does not return to zero. However, a minimum value of 0.059 is observed at the last DANTE pulse ($t = 600$ μs). We refer the time of the minimum to as the "optimized" rephasing time. In our simulation, the "optimized" rephasing time has been adjusted to fall immediately after the last DANTE pulse by changing the value of g.

For the case of the curve by dotted line in Fig. 2a, a minimum value of 0.029 is observed at $t = 1162$ μs (see caption of Fig. 2a). It can be seen by comparing the two distinct minimum values observed at $t = 600$ and 1162 μs that the "optimized" rephasing obtained for the 270° Gaussian modulation is less complete compared to that obtained for the 90° Gaussian modulation followed by the separate rephasing. This is why, in the case of the 270° Gaussian modulation, the two mutually complementary FID's obtainable by applying the negative and positive field gradient must be acquired, as mentioned in the previous section.

The simulation results of in-phase M_y and out-of-phase M_x components of transverse magnetization at the "optimized" rephasing times ($t = 600$ and 1162 μs) are shown in Fig. 2b. Curves are given for the 270° (lower) and 90° (upper) Gaussian modulations. The frequency dependence of M_y can be converted to the spatial dependence, i.e., the profile of the selected slice, by the application of a field gradient. Compared to the latter 90° results, the former 270° results exhibit a much larger residual M_x component and a slightly narrower slice profile accompanied by weak sidelobes. These sidelobes are considered to result from truncation of the Gaussian shape of modulation, because the intensity increases with decreasing factor of g while the excitation time is fixed at 600 μs.

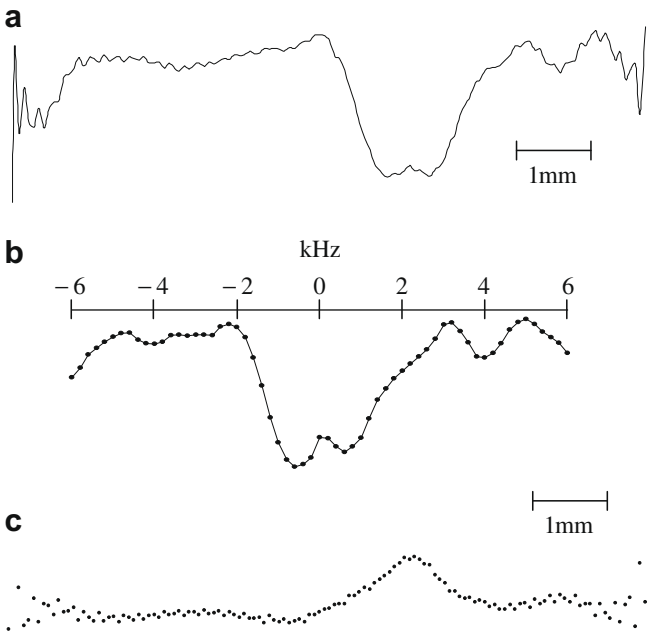

Fig. 3. Experimental slice profiles on adamantane. (a) Profile obtained by the self-refocused ME DANTE with the field gradient. The two complementary signals obtained by monitoring with the positive gradient and the negative gradient (Fig. 1, lower sequence) have been appropriately summed up to form a single profile. (b) Profile observed by the self-refocused ME DANTE without the field gradient. (c) Profile obtained by the conventional ME DANTE using the Gaussian modulation with the field gradient. The peak amplitude is diminished to approximately 48% relative to that of (a) and (b) due to transverse relaxation during the rephasing period. The carrier frequency in the excitation period (Fig. 1) was swept by the step of 0.2 kHz. The main peaks in (a) and (c) are intentionally shifted to the right (2 kHz) by switching the carrier frequency in the monitoring period only for avoiding the central dip artifact. See text for details of the central dip. The beat patterns on both ends in (a) and (c) are due to the oversampling in the monitoring period. One hundred FID's were accumulated in (a) and (c), and ten FID's in (b). These results demonstrate that the slice can be well selected with no rephasing period by the self-refocused ME DANTE sequence. The small sidelobes degrade the selectivity of the slice selection to some extent.

4. Experimental results and discussion

We have conducted two types of self-refocused ME DANTE experiments using a Gaussian modulation with $g = 2.0 \times 10^7$ on test samples of adamantane and polycarbonate; the flip angles were $\alpha_1 = \alpha_6 = 13.8°$, $\alpha_2 = \alpha_5 = 43.6°$ and $\alpha_3 = \alpha_4 = 77.6°$ ($N = 6$). One is the experiment using the positive field gradient and the negative field gradient in the monitoring period (Fig. 1, lower sequence). As pointed out in the previous section, the FID's acquired under the positive and negative field gradient are Fourier transformed and combined into a single data. Thus, a slice profile at the starting point of monitoring can be obtained. The other experiment is made in the absence of the field gradient. A trajectory of a spin isochromat is followed to evaluate the amplitudes of M_y and M_x at the end of the excitation. The frequency of the isochromat is varied; then, the amplitudes are plotted against the frequency. The carrier frequency is swept in the range from −6.0 to +6.0 kHz by the step of 0.2 kHz. The conventional experiments using the 90° flipping Gaussian modulation have also been performed for comparison.

Fig. 3 shows the slice profiles obtained on the sample of adamantane. Fig. 3a and b display the results of the self-refocused experiments; the profile acquired in the presence of the field gradient is represented by solid line and the profile recorded in the absence of the field gradient is depicted by dot-connected line. The profile obtained by the conventional 90° Gaussian modulation is shown by dotted line in Fig. 3c. The peak amplitude is diminished by the transverse relaxation to approximately 48%, compared to those in Fig. 3a and b. The simulations which take into account the relaxation effects by assuming the transverse relaxation time under the line narrowing, 3.5 ms, and the rephasing time, 1.3 ms, indicate a 39% peak amplitude. A possible explanation of the difference between the experimental and simulation amplitudes occurs by considering the line narrowing efficiency degraded by the interference effects due to the 270° DANTE RF pulses. Namely, the difference could be explained by assuming that the transverse relaxation time was shortened from 3.5 to 2.2 ms during the excitation time.

Despite that the profiles in Fig. 3a and b were obtained by the different types of experiments, the profiles appear nearly the same except the artifacts at both ends [1]. The artifacts will be discussed below together with the central dip artifact. The shape and width of the central peak agree with those of the simulation result in Fig. 2b. This demonstrates that the slice is well selected by the self-refocused ME DANTE sequence with no separate rephasing period. The sidelobes at the bases of central peaks, which are considerably stronger than those in the simulation result in Fig. 2b, degrade the selectivity of slice selection by the self-refocused ME DANTE to some extent. The sidelobes on the right are more intense than those on the left. This asymmetry may probably be related to the asymmetric offset dependence of the line narrowing efficiency which was observed by ME experiments. The origin of the asymmetric offset dependence of the line narrowing efficiency has not yet been identified.

Fig. 4 displays the slice profiles obtained on polycarbonate. The appearance of the profiles acquired by the self-refocused method (solid line in Fig. 4a and dot-connected line in Fig. 4b) is generally the same as that of the profiles in Fig. 3, though the artifacts at both ends are prominent in Fig. 4a. For comparison, Fig. 4 further includes the experimental profiles (dotted line) obtained by using the conventional method (Fig. 1, upper sequence) under the same experimental condition. The simulations including the relaxation effects predict a 11% peak amplitude for the profile obtained by the conventional method relative to those acquired by the self-refocused method. The very weak amplitudes are actually observed

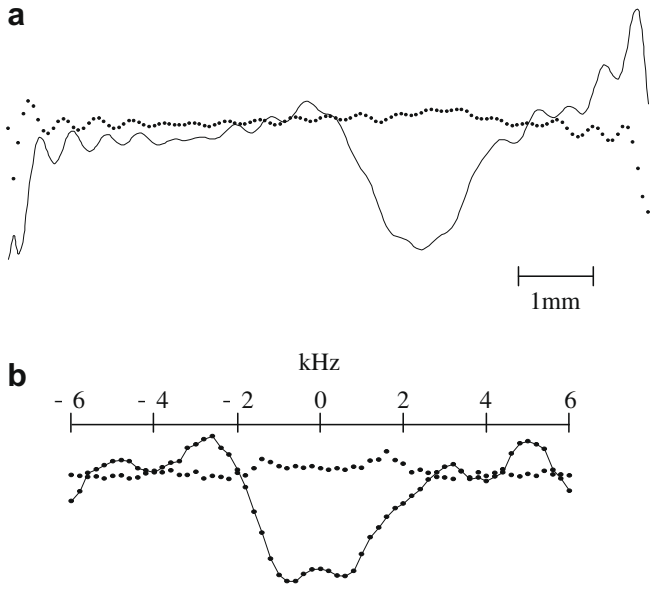

Fig. 4. Experimental slice profiles on polycarbonate. (a) Profiles obtained by the conventional (dotted line) and self-refocused ME DANTE (solid line) sequences with the field gradient (see Fig. 1). (b) Profiles obtained by the conventional (dotted line) and self-refocused ME DANTE (dot-connected line) sequences without the field gradient. These results were obtained under the same experimental condition as for adamantane (Fig. 3). One hundred FID's were accumulated in (a) and ten FID's in (b). It can immediately be seen that the self-refocused method is greatly superior to the conventional method in sensitivity. This remarkable improvement has been brought about by the elimination of the rephasing period.

by the conventional experiments, prohibiting the precise estimate of the relative amplitudes. The relative amplitudes, however, appear to be roughly consistent with the value of 11%. These results clearly demonstrate that the self-refocused method is superior to the conventional method in sensitivity. The signal excited by the conventional method decays down nearly to the noise level during the dephasing period of 1.3 ms. The transverse relaxation time prolonged by the ME sequence was about 0.9 ms for this sample. This is typical for most organic solids.

As mentioned above, the profiles 3b and 4b exhibit a relatively strong dip artifact in the center. This central artifact may mainly be ascribed to the fact that the efficiency of the ME line narrowing abruptly decreases near resonance where the second averaging is ineffective [18]. The central artifact cannot be avoided in the experiment of Figs. 3b and 4b. In the profiles 4a, 3a, and 3c no or only a weak dip artifact is observed. In the experiments for these profiles, the central peaks were intentionally shifted to the right by switching the carrier frequency in the monitoring period while the carrier frequency was set to the on resonance frequency in the excitation period to avoid the central artifact. We have no suitable explanation for the weak dip artifact in the profile 3a at present. These results, however, strongly suggest that the central artifact is mainly due to the monitoring ME sequence. The profiles 3a, 3c, and 4a suffer from another artifact on both sides. The beat patterns with a peak on both ends are due to the oversampling (sampling signal twice the cycle time t_c) in the monitoring period for doubling the FOV.

Finally, it should be added that the profiles in Fig. 4 might suffer from the chemical shift artifact. This is because polycarbonate consists of methyl and phenyl protons which exhibit the relatively large chemical shift difference of 5.5 ppm [10]. However, the difference of 5.5 ppm only amounts to 330 Hz in our low field of 1.4 T. The difference of 330 Hz is further scaled down to 110 Hz under the ME line narrowing. The chemical shift difference thus cannot be resolved by our resolution of about 210–290 Hz (depending on the resonance offset) achieved by TREV8, producing no chemical shift artifact.

5. Conclusions

We have improved the slice selection method for solid-state MRI that we proposed by combining DANTE with the ME line narrowing. The improvement that the rephasing period for recovering dephasing of the excited signal becomes unnecessary can be achieved by introducing self-refocusing effect to the slice selection method. The self-refocusing effect has been implemented successfully by using the 270° flipping Gaussian modulation of DANTE RF pulses in the ME DANTE sequence. This has been demonstrated by the modified ME DANTE experiments performed on the test samples of adamantane and polycarbonate. The superiority to the conventional method in sensitivity was clear particularly in the case of the polycarbonate sample with the short transverse relaxation time under line narrowing. However, the problem of the sidelobes more intense than the simulation remains to be solved. Additional experiments for improving the performance of the ME DANTE method are currently in progress.

6. Experimental

All the experiments were performed on a homebuilt NMR imager, operating at 59.85 MHz for protons. Most experimental conditions were the same as those described previously [1]. The width of the 90° pulses in the ME sequence was 2.4 μs. The flip angles of the DANTE RF pulses were adjusted as described before [1]. Since the total flip angle is three times as large as that of the conventional method, the width of the RF pulse with the largest flip angle 77.6° can be as wide as 2.1 μs, which is not negligibly short. In fact, the timing of application of DANTE RF pulses was quite critical. Even a 1 μs shift resulted in changing the amplitude of sidelobes. This observation could be regarded as a weak interference between the DANTE and ME sequences.

Relaxation times of adamantane were $T_1 \sim 1$ s and $T_2 = 50$ μs, and those of polycarbonate were $T_1 \sim 200$ ms and $T_2 = 30$ μs. The T_2's of adamantane and polycarbonate were prolonged to 3.5 and 0.9 ms respectively by the ME line narrowing (TREV8). The adamantane sample was filled in a 7 mm tube. The bulk polycarbonate sample was cut into a cube which fits inside of the tube. A field gradient of 41 mT/m was applied perpendicular to the tube axis.

Acknowledgment

We thank Mrs. Kazuko Inouye of Institute for Applied Mathematics Inc. for financial support.

References

[1] S. Matsui, H. Masumoto, T. Hashimoto, Tailored slice-selection in solid-state MRI by DANTE under magic-echo line narrowing, J. Magn. Reson. 186 (2007) 238–242.
[2] G. Bodenhausen, R. Freeman, G.A. Morris, A simple pulse sequence for selective excitation in Fourier transform NMR, J. Magn. Reson. 23 (1976) 171–175.
[3] W.-K. Rhim, A. Pines, J.S. Waugh, Time-reversal experiments in dipolar-coupled spin systems, Phys. Rev. B 3 (1971) 684–696.
[4] K. Takegoshi, C.A. McDowell, A "magic echo" pulse sequence for the high-resolution NMR spectra of abundant spins in solids, Chem. Phys. Lett. 116 (1985) 100–104.
[5] S. Matsui, Solid-state NMR imaging by magic sandwich echoes, Chem. Phys. Lett. 179 (1991) 187–190.
[6] S. Matsui, Suppressing the zero-frequency artifact in magic-sandwich-echo proton images of solids, J. Magn. Reson. 98 (1992) 618–621.
[7] S. Matsui, Y. Ogasawara, T. Inouye, Proton images of elastomers by solid-state NMR imaging, J. Magn. Reson. A 105 (1993) 215–218.
[8] S. Matsui, A. Uraoka, T. Inouye, Solid-state NMR imaging by tetrahedral-magic-echo time-suspension sequences, J. Magn. Reson. A 120 (1996) 11–17.

[9] S. Matsui, S. Saito, T. Hashimoto, T. Inouye, NMR second moment imaging using Jeener–Broekaert dipolar signals, J. Magn. Reson. 160 (2003) 13–19. and references therein.
[10] F. Weigand, B. Blümich, H.W. Spiess, Application of nuclear magnetic resonance magic sandwich echo imaging to solid polymers, Solid State NMR 3 (1994) 59–66.
[11] M.L. Buszko, G.E. Maciel, Magnetic-field-gradient-coil system for solid-state MAS and CRAMPS NMR imaging, J. Magn. Reson. A 107 (1994) 151–157.
[12] M.A. Hepp, J.B. Miller, Mapping molecular orientation by solid-state NMR imaging, J. Magn. Reson. A 111 (1994) 62–69.
[13] G.S. Boutis, P. Cappellaro, H. Cho, C. Ramanathan, D.G. Cory, Pulse error compensating symmetric magic-echo trains, J. Magn. Reson. 161 (2003) 132–137.
[14] P.R. Locher, Computer simulation of selective excitation in NMR imaging, Philos. Trans. R. Soc. Lond. B 289 (1980) 537–542.
[15] P.T. Callaghan, Principles of Nuclear Magnetic Resonance Microscopy, Oxford University Press, 1991.
[16] L. Emsley, G. Bodenhausen, Self-refocusing effect of 270° Gaussian pulses. Applications to selective two-dimensional exchange spectroscopy, J. Magn. Reson. 82 (1989) 211–221.
[17] R. Freeman, J. Friedrich, W. Xi-Li, A pulse for all seasons. Fourier transform spectra without a phase gradient, J. Magn. Reson. 79 (1988) 561–567.
[18] D.G. Cory, J.B. Miller, A.N. Garroway, Multiple-pulse methods of ^{1}H NMR imaging of solids: second-averaging, Mol. Phys. 70 (1990) 331–345.